Microstructure of Trabecular Bone in a Mouse Model for Down Syndrome

TRISH PARSONS,[1] TIMOTHY M. RYAN,[1,2] ROGER H. REEVES,[3] AND JOAN T. RICHTSMEIER[1,4]*

[1]Department of Anthropology, Pennsylvania State University, University Park, Pennsylvania
[2]Center for Quantitative Imaging, Pennsylvania State University, University Park, Pennsylvania
[3]Department of Physiology, Johns Hopkins University School of Medicine, Baltimore, Maryland
[4]Centers for Craniofacial Development and Disorders and Functional Anatomy and Evolution, Johns Hopkins University School of Medicine, Baltimore, Maryland

ABSTRACT

Down syndrome (DS) is caused by trisomy of human chromosome 21 (Hsa21) and results in a suite of dysmorphic phenotypes, including effects on the postcranial skeleton and the skull. We have previously demonstrated parallels in the patterns of craniofacial dysmorphology in DS and in the Ts65Dn mouse model for DS. The specific mechanisms underlying the production of these changes in craniofacial shape remain unknown. High-resolution computed tomography scan data were collected for the presphenoid bone of euploid and aneuploid mice. Three-dimensional morphometric parameters of trabecular bone were quantified and compared between euploid and aneuploid mice using nonparametric statistical tests. Aneuploid presphenoid bones were smaller than those of their euploid littermates and had lower bone volume fraction and fewer, more rod-like trabeculae. The differences in cancellous bone structure suggest that bone development, perhaps including bone modeling and remodeling, is affected by aneuploidy. These differences may contribute to the observed dysmorphology of skull and postcranial skeletal phenotypes in DS. Anat Rec, 290:414–421, 2007.

Key words: trabecular bone; Down syndrome; mouse model; high-resolution microcomputed tomography; trisomy 21; presphenoid bone; aneuploidy

Down syndrome is caused by triplication of the genes on human chromosome 21 and results in a variety of characteristic phenotypes that affect nearly all systems of the body (Epstein et al., 1981, 1991; Van Cleve and Cohen 2006; Van Cleve et al., 2006). Several of these DS phenotypes (e.g., atlanto-axial instability, reduced size of limbs, reduced or absent nasal bones, characteristic facial appearance, brachycephaly, microcephaly, flat nasal bridge, brachydactyly, vaulted palate) involve osseous malformations that represent anomalies of the skeletal system. Whether these skeletal phenotypes are individual local anomalies (dysosteochondroses) or are representative of a systemic osseous effect (osteochondrodysplasias) is not known (Mundlos and Olsen, 1997a, 1997b).

Trish Parson's current address is: Faculty of Medicine, University of Calgary, Calgary, Canada.

*Correspondence to: Joan Richtsmeier, Department of Anthropology, Pennsylvania State University, 409 Carpenter Building, University Park, PA 16802. Fax: 814-863-1474. E-mail: jta10@psu.edu

Received 19 July 2006; Accepted 11 November 2007

DOI 10.1002/ar.20494

Published online 27 February 2007 in Wiley InterScience (www.interscience.wiley.com).

Several genetic models for DS have been developed in mice that enable direct examination of specific phenotypes under controlled conditions. These models include the Ts65Dn mouse, which is at dosage imbalance for a marker chromosome that spans 15.6 Mb and contains 136 of the 165 genes shared between Hsa21 and mouse chromosome 16 (Mmu16) (Reeves, 2006), and the Ts1Cje mouse model (Sago et al., 2000), which is trisomic for a segment of Mmu16 that spans 9.8 Mb and includes 104 of the orthologous genes found in Ts65Dn. We used chromosome engineering to produce additional mouse models for aneuploidy that are at dosage imbalance for the mouse orthologs of specific segments of Mmu16 (Olson et al., 2004). Recently, Tc1 mice that contain a nearly intact copy of Hsa21 were described (O'Doherty et al., 2005).

The characteristic mid-face hypoplasia, reduced facial height and reduced bizygomatic breadth measured in DS individuals, results from reduced dimensions of the maxilla, zygomatic, frontal, and nasal bones (Kisling, 1966). These characteristics are recapitulated in the Ts65Dn mouse as demonstrated by a three-dimensional (3D) comparative morphometric analysis of aneuploid and euploid Ts65Dn mice (Richtsmeier et al., 2000). Conservation of the genetic programs regulating skull development is demonstrated by the direct parallel effects produced by the same genetic insult in mouse and human (Reeves et al., 2001). Rather than gross malformations, the craniofacial signature of trisomy of Hsa21 genes and their orthologs results from multiple subtle changes in cranial elements in humans and in mouse models for DS (Richtsmeier et al., 2000, 2002). Individual bones of the skull are affected differentially and there is heightened phenotypic variation in skull morphology among DS individuals and in Ts65Dn aneuploid mice (Richtsmeier et al., 2000). Here we ask whether the difference in skull shape between euploid and aneuploid mice is limited to differential changes in the size and shape of various osseous elements, or if aneuploidy is also associated with changes in bone structure. We do this by conducting the first investigation of trabecular structure in aneuploidy using data from high resolution micro-computed tomography (HRCT) scanning.

Cancellous or trabecular bone differs from compact bone in its gross morphology, anatomical distribution, and mechanical behavior (Swartz et al., 1998). Trabecular bone occurs in the epiphyses and metaphyses of long bones, the centra of vertebra, and in the interior of flat bones, including those of the skull. Bony trabeculae are 3D networks of discrete plates and/or struts interspersed between large marrow spaces. The specific architectural qualities of trabecular bone are affected by a number of factors, including genes, environment, applied loads, nutrition, and infection (Parfitt, 1983; Currey, 1984; Lanyon and Rubin, 1985; Carter et al., 1987; Shimada et al., 1990; Hall, 2005). Several reviews of the molecular processes required for cartilage and bone formation in the skull are available (Wilkie and Morriss-Kay, 2001; Depew et al., 2002; Rossant and Tam, 2002; Francis-West et al., 2003). We also know many of the molecular details of the initiation and organization of skeletogenic cellular condensations, differentiation of those cells, proliferation of the cells of the initial centers, secretion of collagen, and eventual modeling and remodeling of bone (for an exhaustive recent review, see Hall, 2005). To understand the impact of genetic changes on processes that affect bone development, however, equally precise morphological studies are required to quantify morphological variation and determine absolute genotype-phenotype correspondences.

We use the Ts65Dn mouse model to study the impact of trisomy for genes orthologous to those on HSA21 on the architecture of trabecular bone. We utilized HRCT scanning to analyze the trabecular structure of the presphenoid bone of the basicranium in adult euploid and aneuploid mice. Other studies have successfully used this same nondestructive technique to evaluate bone trabeculae in mouse models of bone loss (e.g., Amblard et al., 1998; Abe et al., 2000; Ishijima et al., 2002) and to study differences in trabecular structure among inbred mouse strains (e.g., Beamer et al., 1996; Turner et al., 2000; Martin-Badosa et al., 2003; Ishimori et al., 2006). Though Beamer et al. (1996) determined that more than 70% of the variation in human bone density is attributed to genetic factors, trabecular architecture also adapts to mechanical load via morphogenesis (Lanyon, 1974; Hayes and Snyder, 1981; Radin et al., 1982; Carter et al., 1989; Mullender and Huiskes, 1995; Biewener et al., 1996). Thus, trabecular architecture significantly influences measures of bone strength and density (Ciarelli et al., 1991; Gordon et al., 1996; Siffert et al., 1996; Ulrich et al., 1999). We considered the influence of mechanical load when designing this comparative study.

We have previously demonstrated that trisomy results in specific changes in skull shape and size (Richtsmeier et al., 2000, 2002). Here we examine bone architecture to determine whether segmental trisomy affects the organization and production of bone.

MATERIALS AND METHODS

Mice

Details of animal husbandry for mice used in this study can be found in Richtsmeier et al. (2000). All mice were maintained in a virus- and antibody-free facility with food and water ad libitum and all procedures were approved by the Institutional Animal Care and Use Committee. Ts65Dn mice (B6EiC3H-a/A-Ts65Dn; Jackson Laboratory) were maintained on the B6/C3H background. Mice used in this study were generated by crossing female Ts65Dn aneuploid mice with B6/C3H or CBA/CaJ mice (Jackson Laboratory). Genotypes were determined by karyotyping blood obtained from the retro-orbital sinus (Davisson et al., 1993).

We chose samples of 10 euploid and 10 trisomic mice for this study from mice used in previous studies attempting to age- and sex-match the samples. All mice analyzed were male excepting one female euploid and two trisomic female mice. All specimens were adults. Age of specimens was matched nearly completely between study samples as mice chosen came from a larger sample of littermates. A relatively young female (age = 2.5 months) is included among the euploid mice, while two older females (age = 8.5 months) are included in the trisomic sample. Excluding these outliers, all adult mice ranged in age from 3.8 to 7.5 months.

Bone Imaging and Volume of Interest Determination

All specimens underwent HRCT scanning in the same orientation at the Center for Quantitative Imaging at the Pennsylvania State University using the X-TEK microfocus subsystem of the HD-600 OMNI-X high-resolution X-ray computed tomography system (Bio-Imaging Research, Lincolnshire, IL). Serial cross-sectional scans were collected in the coronal plane with slice thicknesses ranging from 0.0109 to 0.0131 mm (z-dimension). In our samples, slice thickness did not vary systematically between euploid and aneuploid animals as determined by *t*-test ($P = 0.31$). The difference between the minimum and maximum slice thickness (0.0022 mm) is an order of magnitude smaller than the average trabecular thickness in either group. These observations suggest that differences in organism size and, by extension, slice thickness have minimal effects on our results. The field of view was reconstructed to 10.0 mm with a 1,024 × 1,024 pixel grid resulting in a pixel size of 0.010 mm (x- and y-dimension). After scanning, the data were reduced from their original 16-bit format to 8-bit using the software package ImageJ 1.36 (National Institutes of Health).

Although we cannot fully circumvent biomechanical influences on bony architecture, we use the presphenoid bone, an element of the cranial base that is not known to be markedly affected by biomechanical loading, as our volume of interest (VOI) to minimize effects other than genetic contributions (Fig. 1). The various ossification centers that combine to form the cartilaginous model of the cranial base are clearly visible by histological techniques at 15 days postconception (pc) in the mouse, and ossification of the presphenoid bone is evident by 16.5 days pc (Kaufman, 1995). The trabecular architecture of the presphenoid bone is particularly well suited to our goals for several reasons: it is not subject to differential amounts or directions of stress as a result of trisomy; it is not a site of major muscle attachment; and it is relatively easy to isolate on HRCT slice images and in 3D reconstructions of these images. Moreover, given the position of the presphenoid bone within the cranial base, it is reasonable to assume that locomotory or biomechanical stresses either do not play a role or play only a minimal role in determining the morphology (gross and microscopic) of this bone.

The complete trabecular structure of the presphenoid bone of each specimen was defined and used as the VOI in this study (Fig. 2). Delimitation of the VOI for each specimen was accomplished separately by determining a threshold value that separates bone from air; defining those slice images that contain presphenoid bone; and selecting only trabecular bone and excluding all cortical bone from each slice image containing presphenoid architecture. Just as the size of individual presphenoid bones varied among the specimens, the exact threshold value that differentiated bone from nonbone differed among specimens. The scan data were segmented using the iterative algorithm of Ridler and Calvard (1978; Trussell, 1979). Three-dimensional reconstructions of two VOIs are provided in Figure 2. Parameters that fully characterize the trabecular structure were quantified for each specimen using the 3D reconstruction of the presphenoid bony network defined as the VOI. During both scanning and data collection, investigators were blinded from knowing the karyotype of each mouse.

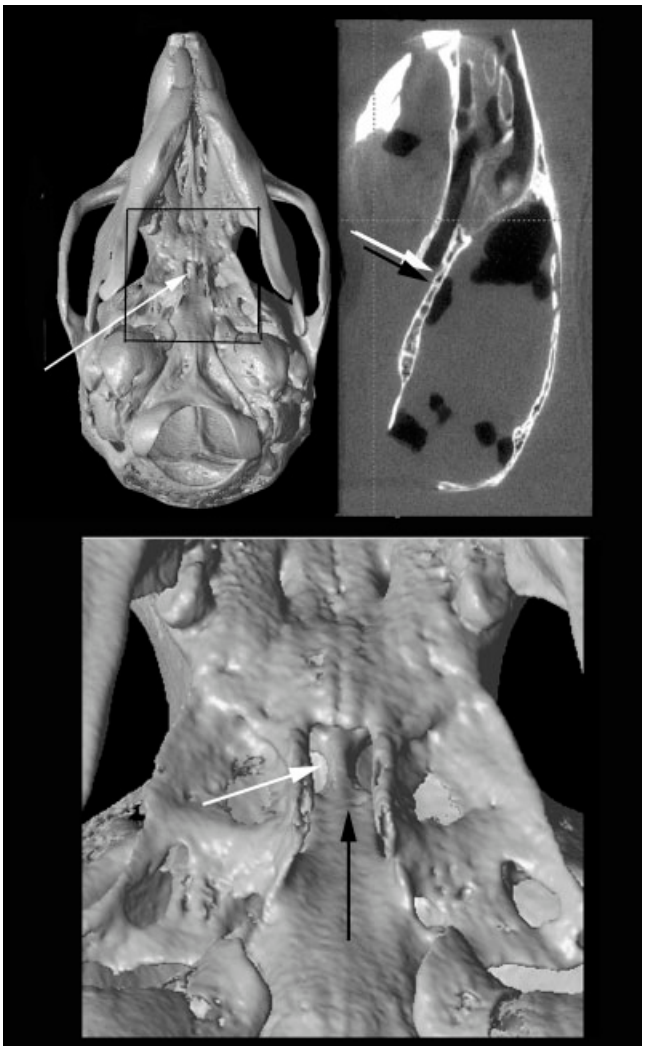

Fig. 1. Position of the presphenoid bone in the mouse basicranium. The upper left is a ventral view of the entire mouse skull, rostrum is at the top, white arrow points to the presphenoid bone, and black box indicates the area shown in the closeup below. At right is a lateral X-ray of the mouse skull, rostrum is at top, white arrow points to the presphenoid bone, while the black arrow points to the suture between the presphenoid (rostral) and the basisphenoid (caudal). Below is a closeup of the 3D reconstruction of HRCT of the ectocranial base, rostrum is at top, white arrow points to the presphenoid bone, while black arrow points to the suture between the presphenoid and basisphenoid.

Morphometric Analysis

Three-dimensional morphometric parameters of trabecular bone were quantified for the entire segmented VOI from each individual using several software packages, including Quant3D (Ryan and Ketcham, 2002; Ketcham and Ryan, 2004), Amira 3.1 (Mercury Computer Systems, San Diego, CA), and custom code written in PV-WAVE (Visual Numerics, Houston, TX). These pa-

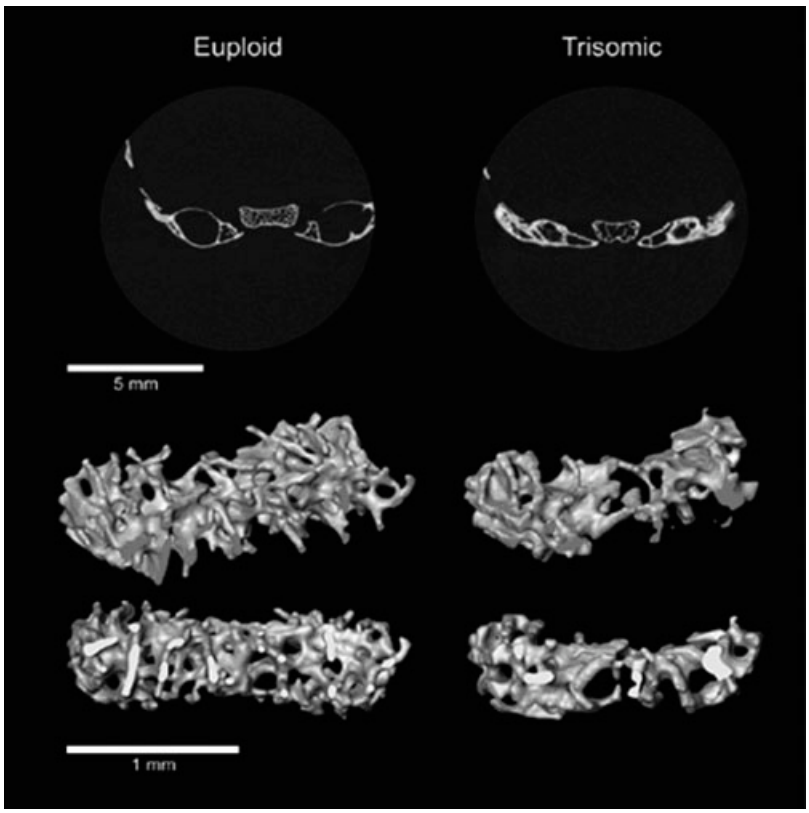

Fig. 2. Three-dimensional trabecular structure of the presphenoid. Top row shows a single coronal cross-sectional HRCT slice image taken through a euploid (left) and a trisomic (right) mouse cranial base. In each slice, the presphenoid bone is centrally located (ectocranial surface is at bottom), surrounded by the bilateral wings of the basi-sphenoid. Three-dimensional reconstructions of the VOI (presphenoid trabecular structure) for a euploid left and a trisomic right mouse are shown in the second (oblique view) and third (anteroposterior view) rows. Cortical bone that would surround the trabeculae of the presphenoid has been excluded from three-dimensional reconstructions.

rameters included bone volume fraction (BV/TV), bone surface-to-volume ratio (BS/BV), trabecular thickness (Tb.Th), trabecular number (Tb.N), fabric anisotropy using the star volume distribution (SVD) method, the structure model index (SMI), and the connectivity density (Conn.D).

The BV/TV was calculated as the ratio of bone volume (BV) to total volume of the VOI after segmentation (TV). The BS/BV parameter was defined as the ratio of bone surface area (BS) to bone volume. Tb.Th was defined as the shortest linear intercept lying entirely within the bone measured at each of 8,000 randomly positioned points lying within the bone phase. Tb.N was calculated by counting the total number of intersections between a linear grid and the bone structure in 3D normalized by total grid line length and is expressed as the number per mm. Conn.D measures the number of interconnections among trabecular and was calculated using the Euler-Poincaré topological approach (Odgaard and Gundersen, 1993). The SMI was determined using the method outlined by Hildebrand and Reugsegger (1997), in which a differential analysis of the triangulated surface of the bone provides a characterization of the proportion of rods and plates in the structure. The SMI fluctuates in value between 0 and 3, depending on the nature of trabecular shape. A value of 0 corresponds with plate-like structures while rods are associated with a value of 3.

The concept of fabric anisotropy describes the distribution of material in 3D (Odgaard, 1997), allowing the characterization of structures as anisotropic, displaying a nonrandom distribution of material, or isotropic, having no detectable material orientation. In the SVD analysis, 8,000 points were randomly placed within each VOI and the longest linear intercept lying within the bone phase (i.e., not intersecting an air space) and passing through the point was measured for 2,049 orientations uniformly distributed in 3D space (Ketcham and Ryan, 2004). The endpoints of each linear intercept are defined by the position at which trabecular bone meets air. Linear intercept and orientation data were compiled into a weighted 3×3 orientation matrix that describes the 3D distribution of trabecular bone within each VOI and the fabric tensor was derived from this matrix (Odgaard et al., 1997; Ketcham and Ryan, 2004).

Eigenanalysis of the fabric tensor provides descriptors of the orientation and magnitude of the major material axes of the VOI, which enables the estimation of anisotropy. The degree of anisotropy (DA) is calculated as the ratio of the first and third eigenvalues, where a value of 1.0 indicates a fully isotropic structure with material equally distributed in all directions, while larger numbers are indicative of more anisotropic structure within the VOI. The elongation index (E) is defined using the equation:

$$E = 1 - \frac{\tau_2}{\tau_1}$$

where τ_1 is the first eigenvalue and τ_2 is the second eigenvalue. Used in combination with DA, E provides another, more specific characterization of the material distribution in 3D.

Statistical Analysis

Once all parameters were measured, the genotype of each individual was revealed and mice were grouped

TABLE 1. Summary of Descriptive and Test Statistics

	Mean	St Dev	CV	Min	Max	*p*
BV/TV						**0.008**
Euploid	0.38	0.09	23.80	0.25	0.51	
Trisomic	0.24	0.08	32.80	0.12	0.36	
BS/BV						0.096
Euploid	48.27	5.31	11.01	39.30	55.27	
Trisomic	54.90	9.37	17.07	48.27	79.78	
TbTh (mm)						0.199
Euploid	0.05	0.01	12.58	0.04	0.06	
Trisomic	0.05	0.003	7.17	0.04	0.05	
Tb.N (/mm)						**0.01**
Euploid	4.37	0.72	16.53	3.22	5.60	
Trisomic	3.57	0.54	15.20	2.83	4.31	
Conn.D (/mm)						**0.019**
Euploid	146.74	53.96	36.77	46.23	218.85	
Trisomic	87.08	94.95	109.04	18.96	336.65	
SMI						**0.019**
Euploid	1.55	0.49	31.42	0.80	2.19	
Trisomic	2.06	0.34	16.41	1.47	2.59	
SVD DA						0.131
Euploid	2.90	1.90	65.73	1.50	7.43	
Trisomic	4.79	3.58	74.84	1.82	13.62	
SVD E						0.082
Euploid	0.29	0.12	42.51	0.10	0.46	
Trisomic	0.44	0.19	42.12	0.19	0.79	

Mean, standard deviation, coefficient of variation, minimum and maximum values for all parameters in the two study samples. *p-values* are reported for non parametric Mann-Whitney U tests for sample differences (SPSS) conducted with euploid listed as the first mean and trisomic as the second. *p-values* for inter sample differences that were determined to be significant ($p \leq 0.05$) are denoted in bold.

into two samples, standard descriptive statistics were calculated for euploid and aneuploid animals, and statistical testing was initiated. Among descriptive statistics, we provide the coefficient of variation (CV), expressed as the ratio of standard deviation to the mean $\times$ 100. CV is a dimensionless number that enables direct comparison of variation of two populations even when means are different. Statistical tests for sample differences were performed using the nonparametric Mann-Whitney U-method (version 14.0; SPSS, Chicago, IL) with 0.05 as the chosen level of significance.

RESULTS

Gross Qualitative Observations

The overall shape of the presphenoid bone differs between euploid and aneuploid mice. Two representative 3D reconstructions from each sample are shown in Figure 2. When examined in cross-section, the euploid presphenoid is rectangular in shape, whereas the trisomic presphenoid bone has rounded inferolateral edges and is compressed along the superoinferior axis at the center.

Quantitative Differences

Descriptive statistics for the study parameters estimated for each group are given in Table 1, along with the results of the Mann-Whitney U-tests. Total volumes (TV) of aneuploid presphenoid bones were also characteristically smaller than those of their euploid littermates as determined by *t*-test ($P = 0.035$). We also applied Levene's test (parametric) and found no difference in variance between euploid and aneuploid mice.

Aneuploid presphenoid bones showed significant differences in trabecular structure for four of the parameters listed in Table 1. Euploid mice have a significantly higher bone volume fraction ($P = 0.008$) and trabecular number ($P = 0.01$) than do trisomic mice (Fig. 3), but BS/BV, Tb.Th, SVD E, and degree of anisotropy (SVD DA) do not differ significantly between the two groups. These results indicate that aneuploid mice have relatively fewer bony struts within the defined VOI, but that those struts do not differ in thickness or anisotropy from those of the euploid mice. The euploid mice have a comparatively greater number of interconnections among trabecular struts (Conn.D). Based on the SMI results, both types of mice have a mixture of rod- and plate-like trabeculae, but the euploid mice appear to have a slightly higher proportion of plates (Fig. 4). In sum, aneuploid mice have fewer trabecular and less bone in the trabecular space. In comparison to euploid mice, aneuploid trabecular bone is more rod-like in shape and does not have as many interconnections with other trabeculae.

DISCUSSION

Assessment of the morphological consequences of genetic anomalies through the quantitative analysis of phenotypes can enable detection of the developmental pathways that are perturbed (e.g., Hallgrímsson and Hall, 2002; Wilkins, 2002; Hallgrímsson et al., 2004). The trabecular structure of the presphenoid bone of Ts65Dn segmentally trisomic mice differs from that of euploid littermates in several ways, which suggest that processes fundamental to bone deposition, and potentially bone resorption, are affected by aneuploidy. Euploid mice appear to produce more trabecular bone relative to aneuploid mice as evidenced by the greater mean bone volume fraction. Connectivity density is substantially larger in euploid mice. Intergroup differences in bone surface to volume ratio and SVD E approach but do not reach significance. Trabecular thickness remains stable regardless of segmental trisomy of 136 genes in aneuploid Ts65Dn mice.

Increased phenotypic variation has been observed in DS relative to the euploid population (Epstein et al., 1991; Hernandez and Fisher, 1999). Increased phenotypic variation in DS individuals has been attributed to "amplified developmental instability," a term that has come to mean that the correct balance of gene expression in pathways regulating development is disrupted by dosage imbalance of the hundreds of genes on Chr21 (Shapiro, 1983, 1997). Such a hypothesis implies that evolutionarily constant developmental trajectories are destabilized by trisomy, resulting in recognizable, though highly variant, phenotypes (Reeves et al., 2001). Although developmental instability as a component of the variable outcome for DS phenotypes makes intuitive sense, the mechanisms that underlie developmental (in)stability and its variation remain poorly understood (Hallgrímsson et al., 2003).

The coefficient of variation (CV) shows increased variation for four of the eight quantitative parameters (Table 1), with ConnD showing a remarkable difference in

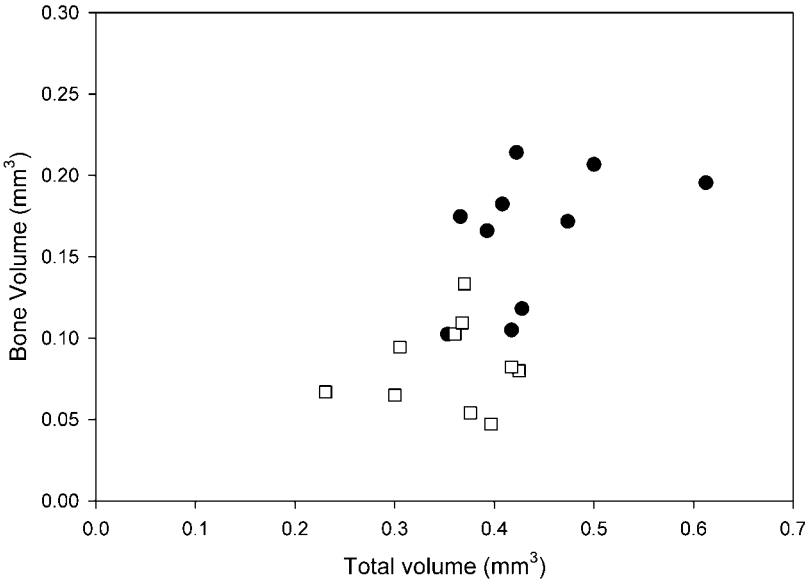

Fig. 3. Bone volume vs. total volume. The relationship between the two parameters used to calculate bone volume fraction (BV/TV) for each specimen are represented. Some overlap is evident between the two groups, however, there is a general separation between the euploid and trisomic mice. This results in a significant difference between groups for the ratio of the two measures. Closed circles denote euploid; open squares, trisomic.

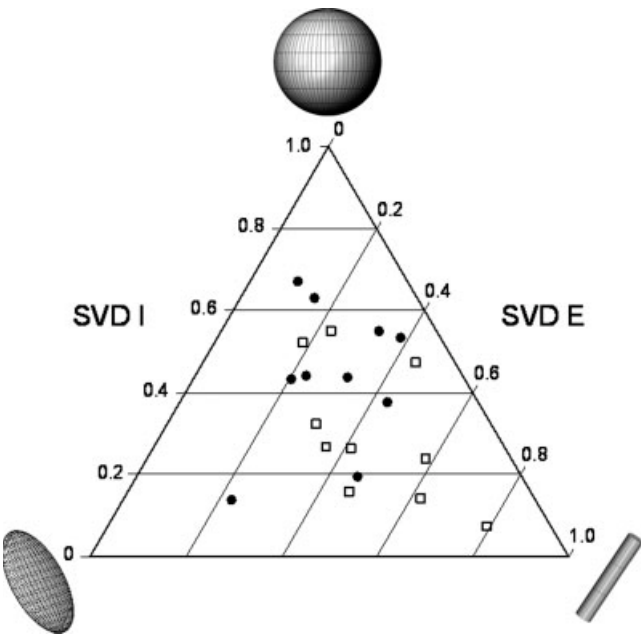

Fig. 4. Ternary shape diagram of fabric anisotropy defined using the star volume distribution method. The elongation index (SVD E) and isotropy index (SVD I) are plotted to show the fabric structure of presphenoid trabecular bone in euploid and trisomic mice. The plot area demonstrates the distributions of trabecular bone structure as a continuum of possible shapes among three extremes. The shapes at the vertices of the triangular plot represent ideal representations of isotropic spheres (eigenvalues approximately equal; top vertex), anisotropic rods (primary eigenvalue $>>$ secondary and tertiary eigenvalues; right vertex), and anisotropic disks or plates (primary eigenvalue $=$ secondary eigenvalue $>>$ tertiary eigenvalue; left vertex). Although there is overlap, euploid trabecular structure tends to be more isotropic while trabeculae of trisomic mice tend to be more anisotropic or unidirectional. Closed circles denote euploid; open squares, trisomic.

variation between euploid and aneuploid mice. Added to previous findings of increased phenotypic variation in aneuploidy, our results suggest that both gross osseous phenotypes and aspects of the microstructures that underlie them are more variable in aneuploid organisms. However, two variables that describe the shape of trabeculae (SMI and Tb.Th) show reduced CV for aneuploid as compared to euploid mice.

Euploid and trisomic mice diverge statistically in body size, with male trisomic mice weighing significantly less than their euploid littermates from the day of birth to adulthood (Roper et al., 2006). Swartz et al. (1998) demonstrated that trabecular size shows little or no dependence on body size in a 2D analysis of mammals ranging in mass from 4 to 40 $\times$ 10^6 g, noting that quite distinct phenomena are dictated by available surface area versus bone volume. A more recent 3D analysis (Fajardo, 2004) also found little size dependence, with only Tb.Th showing a strongly negatively allometric relationship with body mass (slope $=$ 0.05). Importantly, trabecular size can be measured in a number of ways. We found that trabecular thickness does not vary between the two groups but analysis of SMI indicates a difference in the distribution of rods and plates within trabecular bone. Since rods and plates have different 3D morphologies, each has properties pertaining to the amount of surface relative to the overall volume of bone. Though BS/BV and SVD E do not reach our chosen level of significance, the parameter values also suggest intergroup variation in the distribution of rods and plates and the shape of microstructural elements, supporting a tendency toward more rod-like trabeculae in trisomic mice with a greater surface/volume ratio.

We hypothesize that altered construction of bone in trisomic mice is constrained by the requirements of maintaining adequate surface area for calcium homeostasis. It will be informative to investigate both the genetic pathways and developmental events that determine the number of struts formed, as well as constraints

on the degree and nature of variation allowed. Future analyses aimed at the measurement of rates of bone modeling and remodeling may determine whether a difference in calcium metabolism is the basis for these structural differences in the trabeculae of euploid and aneuploid mice.

Our findings could also imply that there is a lower bone mineral density in trisomic mice since less trabeculae may indicate fewer calcium deposits in a given bony region. Reduced mineralization was demonstrated in the humerus, femur, and tibia of ts16 mouse fetuses (Sterz et al., 1989), but our methods were limited to revealing reduced bone mass in Ts65Dn mice. According to the current view on clinical practice in Down syndrome (Van Cleve and Cohen, 2006; Van Cleve et al., 2006), osteopenia and osteoporosis are not common findings in DS. However, Baptista et al. (2005) demonstrated DS to be a risk factor for reduced volumetric bone mineral density of the lower lumbar spine and reduced femoral neck strength in young adults. Since a number of risk factors known to be associated with osteoporosis are common in the DS population, it is unknown whether these factors or trisomy of Chr21 genes underlie the observations of Baptista et al. (2005). Bone mineral density tests are needed to determine if segmentally trisomic Ts65Dn mice show mineralization patterns that are different from normal.

The presphenoid bone should not experience differing biomechanical influences between euploid and trisomic samples. Consequently, our findings suggest a fundamental difference in the formation of trabecular bone in trisomic and euploid mice. We hypothesize that minimal requirements of calcium homeostasis constrain the potential changes in trabecular architecture that are possible, and that changes in bone architecture (and in the processes that produce these changes) contribute to the observed and characteristic differences in skull shape between euploid and aneuploid animals. We previously demonstrated that the skulls of Ts65Dn aneuploid mice differ from euploid skulls in ways that parallel the differences noted between euploid individuals and those with DS and concluded that the altered developmental processes responsible for these differences are accurately reflected in Ts65Dn and Ts1Cje trisomic mice (Richtsmeier et al., 2000, 2002). Thus, the microstructural differences demonstrated here in Ts65Dn mice might be seen in the human condition as well, providing a model to elucidate developmental mechanisms that can be applied to understanding the distinctive skull phenotypes produced by trisomy 21.

ACKNOWLEDGMENTS

Supported by Public Health Service awards 1 P60 DE13078, F33 DE05706-02 (to J.R.), and HD24605 (to R.H.R.).

LITERATURE CITED

Abe S, Watanabe H, Hirayama A, Shibuya E, Hashimoto M, Ide Y. 2000. Morphological study of the femur in osteopetrotic (op/op) mice using microcomputed tomography. Br J Radiol 73:1078–1082.

Amblard D, Lafage-Proust M, Alexandre C, Vico L. 1998. Tail suspension results in stimulation of bone cellular activities without bone loss in high bone mass C3H/HeJ mice: comparison with low bone mass C57BL/6J mice. Bone 23:S510.

Baptista F, Varela A, Sardinha LB. 2005. Bone mineral mass in males and females with and without Down syndrome. Osteoporos Int 16:380–388.

Beamer WG, Donahue LR, Rosen CJ, Baylink DJ. 1996. Genetic variability in adult bone density among inbred strains of mice. Bone 18:397–403.

Biewener AA, Fazzalari NL, Konieczynski DD, Baudinette RV. 1996. Adaptive changes in trabecular architecture in relation to functional strain patterns and disuse. Bone 19:1–8.

Carter DR, Fyhrie DP, Whalen RT. 1987. Trabecular bone density and loading history: regulation of connective tissue biology by mechanical energy. J Biomech 20:785–794.

Carter DR, Orr TE, Fyhrie DP. 1989. Relationships between loading history and femoral cancellous bone architecture. J Biomech 22:231–244.

Ciarelli MJ, Goldstein SA, Kuhn JL, Cody DD, Brown MB. 1991. Evaluation of orthogonal mechanical-properties and density of human trabecular bone from the major metaphyseal regions with materials testing and computed-tomography. J Orthopaed Res 9:674–682.

Currey J. 1984. The mechanical adaptations of bones. Princeton, NJ: Princeton University Press.

Davisson M, Schmidt C, Reeves N, Irving E, Akeson E, Harris B, Bronson R. 1993. Segmental trisomy as a mouse model for Down syndrome. Prog Clin Biol Res 384:117–133.

Depew MJ, Tucker AS, Sharpe PT. 2002. Craniofacial development. In: Rossant J, Tam PPL, editors. Mouse development: patterning, morphogensis, and organogenesis. San Diego, CA: Academic Press. pp 421–498.

Epstein CJ, Epstein LB, Cox DR, Weil J. 1981. Functional implications of gene dosage effects in trisomy 21. Hum Genet 2(Suppl):155–172.

Epstein CJ, Korenberg JR, Anneren G, et al. 1991. Protocols to establish genotype-phenotype correlations in Down syndrome. Am J Hum Genet 49:207–235.

Fajardo RJ. 2004.Comparative microCT analysis of anthropoid trabecular architecture. PhD dissertation. Stony Brook, NY: Stony Brook University.

Francis-West PH, Robson L, Evans DJR. 2003. Craniofacial development: the tissue and molecular interactions that control development of the head. Berlin: Springer.

Gordon CL, Webber CE, Adachi JD, Christoforou N. 1996. In vivo assessment of trabecular bone structure at the distal radius from high-resolution computed tomography images. Phys Med Biol 41:495–508.

Hall BK. 2005. Bones and cartilage: developmental and evolutionary skeletal biology. San Diego, CA: Elsevier Academic Press.

Hallgrímsson B, Hall B. 2002. Modularity within and among limbs: implications for evolutionary divergence in fore- and hind limb morphology in primates. Am J Phys Anthropol 34(Suppl):81.

Hallgrímsson B, Miyake T, Wilmore K, Hall BK. 2003. Embryological origins of developmental stability: size, shape and fluctuating asymmetry in prenatal random bred mice. J Exp Zool 296B:40–57.

Hallgrímsson B, Willmore K, Dorval C, Cooper DM. 2004. Craniofacial variability and modularity in macaques and mice. J Exp Zoolog Part B Mol Dev Evol 302:207–225.

Hayes WC, Snyder B. 1981. Toward a quantitative formulation of Wolff's law in trabecular bone. In: Cowin SC, editor. Mechanical properties of bone. New York: American Society of Mechanical Engineers. p 43–68.

Hernandez D, Fisher E. 1999. Mouse autosomal trisomy two's company three's a crowd. Trends Genet 15:241–247.

Hildebrand T, Ruegsegger . 1997. A new method for the model-independent assessment of thickness in three-dimensional images. J Microsc 185:67–75.

Ishijima M, Tsuji K, Rittling SR, Yamashita T, Kurosawa H, Denhardt DT, Nifuji A, Noda M. 2002. Resistance to unloading-induced three-dimensional bone loss in osteopontin-deficient mice. J Bone Miner Res 17:661–667.

Ishimori N, Li R, Walsh KA, et al. 2006. Quantitative trait loci that determine BMD in C57BL/6J and 129S1/SvImJ inbred mice. J Bone Miner Res 21:105–112.

Kaufman M. 1995. The atlas of mouse development. London: Academic Press.
Ketcham RA, Ryan TM. 2004. Quantification of anisotropy in trabecular bone. J Microsc 213:158–171.
Kisling E. 1966. Cranial morphology in Down's syndrome: a comparative roentgencephalometric study in adult males. Copenhagen: Munksgaard.
Lanyon L. 1974. Experimental support for the trajectorial theory of bone structure. J Bone Joint Surg 56B:160–166.
Lanyon L, Rubin C. 1985. Functional adaptation in skeletal structures. In: Hildebrand D, Bramble K, Liem F, Wake D, editors. Functional vertebrate morphology. Cambridge, MA: Harvard University Press. pp 1–25.
Martin-Badosa E, Amblard D, Nuzzo S, Elmoutaouakkil A, Vico L, Peyrin F. 2003. Excised bone structures in mice: imaging at three-dimensional synchrotron radiation micro CT. Radiology 229:921–928.
Mullender MG, Huiskes R. 1995. Proposal for the regulatory mechanism of Wolff's law. J Orthop Res 13:503–512.
Mundlos S, Olsen BR. 1997a. Heritable diseases of the skeleton: I, molecular insights into skeletal development-transcription factors and signaling pathways. FASEB J 11:125–132.
Mundlos S, Olsen BR. 1997b. Heritable diseases of the skeleton: II, molecular insights into skeletal development-matrix components and their homeostasis. FASEB J 11:227–233.
Odgaard A, Gundersen HJG. 1993. Quantification of connectivity in cancellous bone, with special emphasis on 3-d reconstruction. Bone 14:173–182.
Odgaard A. 1997. Three-dimensional methods for quantification of cancellous bone architecture. Bone 20:315–328.
Odgaard A, Kabel J, van Rietbergen B, Dalstra M, Huiskes R. 1997. Fabric and elastic principal directions of cancellous bone are closely related. J Biomech 30:487–495.
O'Doherty A, Ruf S, Mulligan C, et al. 2005. An aneuploid mouse strain carrying human chromosome 21 with Down syndrome phenotypes. Science 309:2033–2037.
Olson L, Richtsmeier JT, Leszl J, Reeves R. 2004. A chromosome 21 critical region does not cause specific Down syndrome phenotypes. Science 306:687–690.
Parfitt AM. 1983. Recent developments in bone physiology. Henry Ford Hosp Med J 31:209–210.
Radin EL, Orr RB, Kelman JL, Paul IL, Rose RM. 1982. Effect of prolonged walking on concrete on the knees of sheep. J Biomech 15:487–492.
Reeves RH, Baxter LL, Richtsmeier JT. 2001. Too much of a good thing: mechanisms of gene action in Down syndrome. Trends Genet 17:83–88.
Reeves R. 2006. Down syndrome mouse models are looking up. Trends Mol Med 12(6): 237–240.
Richtsmeier JT, Baxter LL, Reeves RH. 2000. Parallels of craniofacial maldevelopment in Down syndrome and Ts65Dn mice. Dev Dyn 217:137–145.
Richtsmeier JT, Zumwalt A, Carlson EJ, Epstein CJ, Reeves RH. 2002. Craniofacial phenotypes in segmentally trisomic mouse models for Down syndrome. Am J Med Genet 107:317–324.
Ridler T, Calvard S. 1978. Picture thresholding using an iterative selection method. IEEE Trans Syst Man Cybernet 13:231–235.
Roper RJ, St John HK, Philip J, Lawler A, Reeves RH. 2006. Perinatal loss of Ts65Dn Down syndrome mice. Genetics 172:437–443.
Rossant J, Tam P, editors. 2002. Mouse development: patterning, morphogenesis, and organogenesis. San Diego, CA: Academic Press.
Ryan TM, Ketcham RA. 2002. Femoral head trabecular bone structure in two omomyid primates. J Hum Ecol 43:241–263.
Sago H, Carlson E, Smith D, Rubin E, Crnic L, Huang T, Epstein C. 2000. Genetic dissection of region associated with behavioral abnormalities in mouse models for Down syndrome. Pediatr Res 48:606–613.
Shapiro B. 1983. Down syndrome: a disruption of homeostasis. Am J Med Genet 14:241–269.
Shapiro B. 1997. Whither Down syndrome critical regions? Hum Genet 99:421–423.
Shimada S, Yamaguchi N, Honda Y. 1990. Eustachian tube function and mastoid pneumatization. Acta Otolaryngol 471(Suppl):51–55.
Siffert RS, Luo GM, Cowin SC, Kaufman JJ. 1996. Dynamic relationships of trabecular bone density, architecture, and strength in a computational model of osteopenia. Bone 18:197–206.
Sterz H, Buselmaier W, Bacchus C, Gromier L, Eppler E. 1989. Defects of skeletal morphology, density, and structure in mouse fetuses with trisomy 16. Teratology 40:627–639.
Swartz S, Parker A, Huo C. 1998. Theroetical and empirical scaling patterns and topological homology in bone trabeculae. J Exp Biol 201:573–590.
Trussell HJ. 1979. Comments on "picture thresholding using an iterative selection method." IEEE Transact Syst Man Cybernet 9:311.
Turner CH, Hsieh YF, Muller R, Bouxsein ML, Baylink DJ, Rosen CJ, Grynpas MD, Donahue LR, Beamer WG. 2000. Genetic regulation of cortical and trabecular bone strength and microstructure in inbred strains of mice. J Bone Miner Res 15:1126–1131.
Ulrich D, van Rietbergen B, Laib A, Rüegsegger P. 1999. The ability of three-dimensional structural indices to reflect mechanical aspects of trabecular bone. Bone 25:55–60.
Van Cleve S, Cohen W. 2006. Clinical practice guidelines for children with Down syndrome from birth to 12 years. J Pediatr Health Care 20:47–54.
Van Cleve S, Cannon S, Cohen W. 2006. Clinical practice guidelines for adolescents and young adults with Down syndrome: 12 to 21 years. J Pediatr Health Care 20:198–205.
Wilkie AO, Morriss-Kay GM. 2001. Genetics of craniofacial development and malformation. Nat Rev Genet 2:458–468.
Wilkins A. 2002. The evolution of developmental pathways. Sunderland, MA: Sinaer Associates.